PHYSICAL REVIEW C VOLUME 54, NUMBER 4 OCTOBER 1996

Cross-section measurements for the ^{2}H$(p,n)2p$ reaction at 135 MeV

B. D. Anderson,[1] A. R. Baldwin,[1] W. Bertozzi,[2] T. N. Buti,[2,*] A. Fazely,[1,3] J. M. Finn,[4] C. C. Foster,[5] W. Glöckle,[6] J. Golak,[7] M. A. Kovash,[2,8] R. Kurmanov,[1,9] R. Madey,[1,10] B. Murdoch,[2,†] P. C. Tandy,[1] J. W. Watson,[1] and H. Witała[7]

[1]*Department of Physics and Center for Nuclear Research, Kent State University, Kent, Ohio 44242*

[2]*Department of Physics, Massachusetts Institute of Technology, Cambridge, Massachusetts 02139*

[3]*Department of Physics, Southern University, Baton Rouge, Louisiana 70808*

[4]*Department of Physics, College of William and Mary, Williamsburg, Virginia 23185*

[5]*Indiana University Cyclotron Facility, Bloomington, Indiana 47405*

[6]*Institut für Theoretische Physik II, Ruhr-Universität Bochum, D-4630 Bochum, Germany*

[7]*Institute of Physics, Jagellonian University, Reymonta 4, PL-30059 Cracow, Poland*

[8]*Department of Physics, University of Kentucky, Lexington, Kentucky 40506*

[9]*Department of Physics and Chemistry, Omsk State Railway Academy, 644046 Omsk, Russia*

[10]*Department of Physics and Research Center for Nuclear and High Energy Physics, Hampton University, Hampton, Virginia 23668*

(Received 3 May 1996)

Cross-section excitation-energy spectra and angular distributions were measured for the ^{2}H$(p,n)2p$ reaction at 135 MeV in 6° steps from 0° to 30° (laboratory), using the beam swinger facility at the Indiana University Cyclotron Facility. The target was a 12.8 mg/cm^2 foil of CD$_2$. Neutron energies were measured by the time-of-flight method using large-volume plastic scintillator arrays at flight paths of 91 m. The overall energy resolution was 260 keV. The 0° spectrum is dominated by a large peak near 0 MeV of relative energy in the final $2p$ system; this peak corresponds to the two protons in the $^1S_0$ state. The wider-angle spectra are dominated by a broad peak centered at 10 to 20 MeV of excitation which is the quasifree scattering peak. The spectra are compared with impulse approximation and three-body Faddeev calculations.
[S0556-2813(96)06510-7]

PACS number(s): 21.45.+v, 24.10.Eq, 25.40.Kv, 27.10.+h

I. INTRODUCTION

The three-nucleon ($3N$) system provides important tests for the study of the nucleon-nucleon (NN) interaction. We present here new measurements of the neutron energy spectrum from the ^{2}H$(p,n)2p$ reaction at 135 MeV. The measurements are compared to Faddeev calculations performed for the conditions of the present experiment. Earlier measurements for this reaction were performed at forward angles only and primarily at lower energies [1–4]. The present measurements extend out to 30°, and the energy resolution (260 keV) is more than two times better than previously obtained for this reaction above 100 MeV. The measurements reported here are for cross sections only and represent the first step in a series of experiments planned for this reaction above 100 MeV. Later measurements will include complete sets of spin observables as well. Comparisons with three-body Faddeev calculations were unavailable for the earlier measurements since such calculations have only recently become possible above 100 MeV.

In the absence of Faddeev calculations above about 100 MeV, the theoretical analysis of three nucleon breakup has usually relied upon approximate methods, such as the impulse approximation, borrowed from nuclear reaction theory. We compare also with such calculations to provide some continuity with recent work of that type [3,4] and also to illustrate qualitatively the dominant mechanisms involved. From this nuclear reaction perspective, the process here is a simple nucleon-induced transition of the target from a deuteron state to a continuum two-proton state. The extreme low-energy portion of the excitation-energy spectrum (the high-energy portion of the neutron-energy spectrum) must be dominated by the $^1S_0$ state because of the Pauli principle. This final-state interaction (FSI) is observed as a large, narrow peak at an excitation energy near 0 MeV. At higher excitation energy one expects that quasifree scattering (QFS), i.e., the (p,pn) reaction should be significant also. This process is observed as a broad peak in the measurements. As we show below, the qualitative features of both of these processes can be described by separate single-step, impulse approximation (IA) calculations. It is significant, however, that both of these processes are described simultaneously by three-body Faddeev calculations. The Faddeev calculations automatically include rescattering to all orders, so that the reaction mechanism is described accurately. This work provides important tests of these calculations.

Three-body Faddeev calculations include both final-state interaction and quasifree scattering mechanisms together with all orders of multiple scattering. Such calculations, with enough partial waves to be realistic up to 200 MeV, are now available [5–7]. Presently, it is not possible to solve the $3N$ Faddeev equations above the deuteron breakup threshold with realistic NN interactions while including exactly the Coulomb force between the two protons; accordingly, the

*Present address: IBM, Route 52, Hope Well Junction, NY 12533.

†Present address: Tektronix Inc., P.O. Box 500, Beaverton, OR 97077.

Faddeev calculations were performed for the analog reaction ^{2}H$(n,p)2n$, to avoid the uncertainties associated with including the long-range Coulomb force in this approach. The importance of the Coulomb interaction for the pp final-state interaction region is shown by comparison to the impulse approximation calculations. Also, the importance of higher-order rescattering for the transition to the final state in the low-energy portion of the excitation-energy spectrum is presented and discussed.

II. EXPERIMENTAL PROCEDURE

The experiment was performed at the Indiana University Cyclotron Facility (IUCF) with the beam-swinger system. The experimental arrangement and data reduction procedures were similar to those described previously [8,9]. Neutron kinetic energies were measured by the time-of-flight (TOF) technique. A beam of 135 MeV protons was obtained from the cyclotron in narrow beam bursts typically 350 ps long, separated by $\approx$230 ns. Neutrons were detected in two detector stations at 0° and 24° with respect to the undeflected proton beam. The flight paths were 91.0 and 90.8 m ($\pm$0.2 m), respectively. The neutron detectors were rectangular bars of fast plastic scintillator 10.2-cm thick. Two separate detectors each 1.02-m long by 0.25-m high were combined for a total frontal area of 0.52 m^2 in the 0° station. The 24° station had two detectors each 1.02-m long by 0.52-m high for a total frontal area of 1.04 m^2. Each neutron detector had tapered Plexiglass light pipes attached on the two ends of the scintillator bar, coupled to 12.8-cm diameter phototubes. Timing signals were derived from each end and combined in a mean-timer circuit [10] to provide the timing signal from each detector. Overall time resolutions of about 825 ps were obtained, including contributions from the beam burst width ($\approx$350 ps), the beam-energy spread ($\approx$400 ps), energy loss in the target ($\approx$300 ps), neutron transit times across the 10.2-cm thickness of the detectors ($\approx$530 ps), and the intrinsic time dispersion of each detector ($\approx$300 ps). This overall time resolution provided an energy resolution of about 260 keV. The large-volume detectors were described in more detail previously [11]. Protons from the target were rejected by anticoincidence detectors in front of each neutron detector array. Cosmic rays were vetoed by anticoincidence detectors on top of each array as well as by the ones at the front.

The target was a self-supporting foil of CD_2, 12.8-mg/cm^2 thick. Spectra were obtained in 6° steps from 0° to 30°. Spectra from each detector were recorded at many pulse-height thresholds from 25 to 90 MeV equivalent-electron energy (MeVee). Calibration of the pulse-height response of each of the detectors was performed with a ^{228}Th source (E_γ = 2.61 MeV) and a calibrated fast amplifier. The values of the cross sections extracted for different thresholds were found to be the same within statistics. The values of the cross sections reported here are at a threshold setting of 40 MeVee.

III. DATA REDUCTION

Excitation-energy spectra were obtained from the measured TOF spectra using the known flight paths and a calibration of the time-to-amplitude converter. Transitions to known states in ^{12}N from the ^{12}C$(p,n)^{12}$N reaction provided absolute reference points. Excitation energy in the p-p final state system is estimated to be accurate to $\pm$0.1 MeV. Excitation-energy spectra from the CD_2 target are shown at three angles in Fig. 1. In order to obtain excitation-energy spectra for the ^{2}H$(p,n)2p$ reaction alone, it was necessary to subtract the contributions from the carbon in the CD_2 target. This was performed in the TOF spectra by subtracting separate runs performed using a self-supporting carbon target. The TOF spectra were aligned using the strong ^{12}C $(p,n)^{12}$N peaks. The carbon-target runs were normalized to the CD_2 runs by comparing yields in the ^{12}C(p,n) peaks. Because there was slightly more energy loss in the CD_2 target than in the carbon target, it was observed that the peaks in the carbon-target runs were slightly narrower than in the CD_2 runs. This difference produced positive and negative swinging oscillations for subtractions of peaks, even when properly aligned and normalized. This problem was eliminated to first order by performing a Gaussian smearing of the carbon-target runs to broaden the TOF peaks. Because of the difference in reaction Q values, these subtraction problems do not interfere with the strong final-state interaction peak in the ^{2}H$(p,n)2p$ reaction, except at the widest angles. Generally, the only real problem from this subtraction is for the strong ^{12}C$(p,n)^{12}$N(g.s) transition at forward angles. Because even with reshaping of the carbon spectra some spurious oscillations remain near this strong peak, we simply omit this part (1 MeV) of the spectra at forward angles. These regions occur only in the continuum part of the ^{2}H$(p,n)2p$ spectra and are not a significant problem for this work.

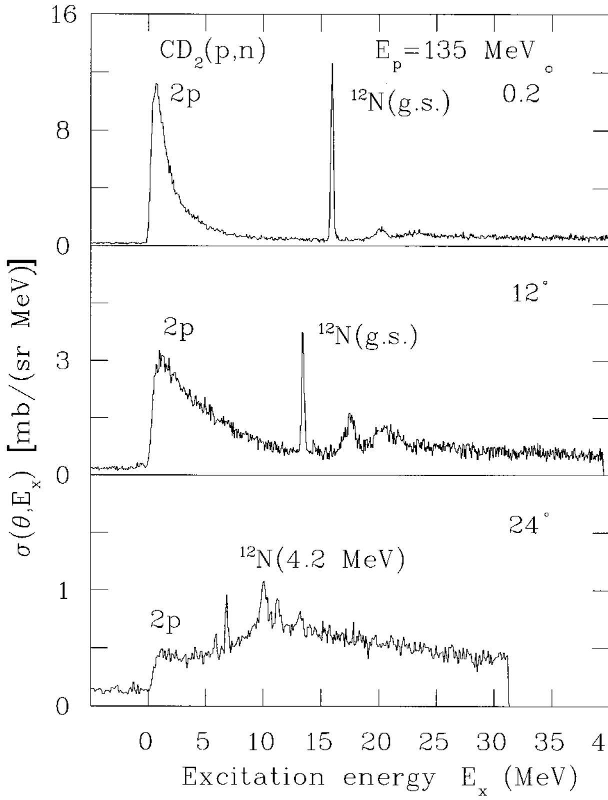

FIG. 1. Excitation-energy spectra for the (p,n) reaction on a CD_2 target at 0.2°, 12°, and 24° at 135 MeV.

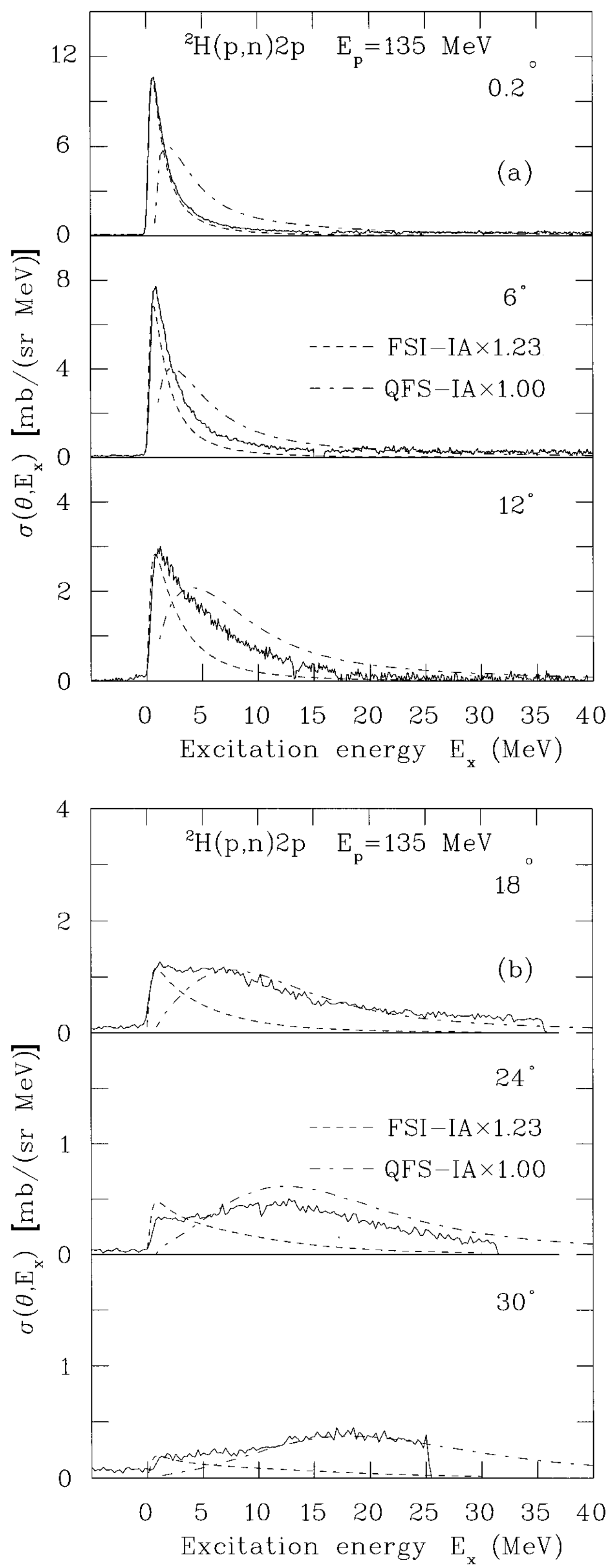

FIG. 2. Comparison of impulse-approximation calculations for the ^{2}H(p,n) reaction to the experimental excitation-energy spectra at (a) 0.2°, 6°, and 12°, and (b) 18°, 24°, and 30°.

Absolute double-differential cross sections were obtained by combining the experimental yields with the measured target thickness, the known flight path, the integrated beam charge, and calculated neutron detector efficiencies [12]. The efficiency calculations have been tested for these detectors at these neutron energies [13,14]. The experimental procedure and data reduction is similar to that described in more detail in Refs. [8] and [9]. The uncertainty in the overall scale factor is dominated by the uncertainty in the detector efficiencies and is estimated to be $\pm 12\%$.

The resulting excitation-energy spectra for the ^{2}H$(p,n)2p$ reaction at 135 MeV are shown in Fig. 2.

IV. COMPARISON WITH IMPULSE-APPROXIMATION CALCULATIONS

We begin by comparing the experimental spectra with impulse approximation (IA) calculations for the two processes that are expected to dominate the ^{2}H$(p,n)2p$ reaction at these energies. These two processes were discussed above and are the transition to the ^{1}S$_0$ final-state interaction (FSI) in the $2p$ system and quasifree pn scattering (QFS).

A. Background: The impulse approximation calculations

The transition to the $^1S_0$ state is expected to dominate in the low excitation-energy region of the $2p$ final state at forward angles. This transition is predominantly from the $^3S_1$ part of the deuteron wave function. Because this transition is S state to S state, it is $\Delta L=0$, and is expected to be peaked at 0°. We calculate this transition in the factorized plane-wave IA with the expression [1–3,15]

$$\frac{d^2\sigma}{d\Omega_n dE_n}=\frac{1}{3}\frac{M_n}{\pi^2}\frac{k_{2p}k_n^L}{k_p}\sigma_{np}|F(q)|^2, \tag{1}$$

where the transition form factor is

$$F(q)=\langle\Phi_{2p}(E_{2p},\vec{r})|e^{i\vec{q}\cdot\vec{r}/2}|\Phi_d(\vec{r})\rangle. \tag{2}$$

Here M_n is the nucleon mass and k_{2p}, k_p, and k_n^L are the relative momenta of the two protons in the final state, of the incident proton in the c.m. system, and of the outgoing neutron in the laboratory system, respectively. The differential cross section, σ_{np}, is the cross section for free n-p scattering at 135 MeV, obtained from the phase-shifts of Arndt [16]. The deuteron wave function, Φ_d, is taken to be a Hulthén-type deuteron wave function [17], and q is the momentum transfer. The final-state $2p$ wave function, Φ_{2p}, is obtained by solving the Schrödinger equation for the $^1S_0$ N-N system with a Reid soft-core potential. The Coulomb interaction is included in the final-state interaction.

It has been shown that quasifree scattering dominates the continuum for inelastic scattering of medium energy protons on nuclei [18]. We expect to see this process in this reaction as a broad kinematic bump, which will move to higher excitation energy with increasing angle. We calculated this process, viz., the (p,pn) reaction, for this case using the plane-wave IA code originally due to Wu [19]. The double-differential cross section is calculated from the expression

$$\frac{d^2\sigma}{d\Omega_n dE_n}=\frac{1}{(\hbar c)^2}\frac{p_n}{p_p|p_p-p_n|}\times\int_{q^{\min}}^{q^{\max}}\int_0^{2\pi}\frac{q\,dq}{E_q}|\Phi_d(q)|^2E_c^2\sigma_{np}d\phi. \tag{3}$$

Here p_p, p_n, and q are the momenta of the incident proton, the emitted neutron, and of the struck nucleon, respectively; E_q is the energy of the struck nucleon, and E_c is the total c.m. energy; ϕ is the angle of revolution around $\vec{p}_p - \vec{p}_n$, measured from the plane formed by $\vec{p}_p - \vec{p}_n$ and $\vec{p}_p$. σ_{np} is the free n-p cross section and $\Phi_d(q)$ is the Fourier transform of the deuteron wave function. The integral is over the momentum of the unobserved nucleon, without any final-state interaction, i.e., the scattering is ''free'' (the binding energy is taken into account). The deuteron wave function is generated using a bound-state subroutine written by Chant [20].

B. Comparison with the IA calculations

In Fig. 2 we show the comparison of the IA calculations with the experimental excitation-energy spectra. In this system the plane-wave IA mechanism is too simplistic to reproduce the absolute magnitude of the cross section. Significant contributions from multiple scattering are missed as shown by later comparison with the Faddeev calculations. Our interest is in whether the IA can capture the dependence upon scattering angle and excitation energy. The normalization factor required for the final-state interaction impulse approximation (FSI-IA) calculation is 1.23, slightly larger than that found by Sakai *et al.* (viz. 1.15) for a similar calculation compared to this same reaction at 120 MeV [3]. Although it is unusual to require a normalization factor greater than unity for a theoretical calculation, for such a ''light'' nucleus, the effects of multiple scattering are not obvious. This is discussed more fully below in Sec. V for the comparisons with Faddeev calculations. At the most forward angles, the spectra are dominated by the $^1S_0$ final-state interaction peak near 0 MeV of excitation. This peak is described well by the final-state interaction (FSI) impulse approximation calculations described above. As one proceeds to larger angles, this peak becomes just a bump near 0 MeV in the continuum spectra. The FSI-IA calculations still are able to describe this bump well, even out to the largest angle available here (viz. 30°).

The quasifree scattering impulse-approximation (QFS-IA) calculation is shown also in Fig. 2. At the most forward angles, one sees that this calculation is in poor agreement with the experimental spectra, but that at wider angles, it describes well the higher-energy part of the spectra; in particular, it reproduces the broad bump seen in the spectra, which slowly moves to higher excitation energy with increasing angle. This bump is the QFS bump and is reproduced by this calculation, with no renormalization factor required. The QFS-IA calculation fails at the forward angles where the FSI peak dominates because this interaction is not included in the QFS-IA calculation. It is significant that the plane-wave QFS-IA calculation is able to describe the absolute magnitude of the wider-angle spectra so well, where there is good kinematic separation of the FSI and QFS mechanisms.

It is not surprising that the IA calculations do not describe the data well at intermediate angles, where both the FSI and QFS amplitudes are large and likely interfere strongly. Of course, this interference cannot be considered easily without a more comprehensive framework for the reaction mechanism. This is one of the reasons that the three-body Faddeev calculations are important, because all of the different mechanisms are essentially considered simultaneously.

V. THREE-BODY, FADDEEV CALCULATIONS

Rigorous solutions of the $3N$ Faddeev equations based on modern, realistic NN interactions have become available [5–7]. The multiple scattering series for three nucleons interacting through pairwise forces and propagating freely in between is summed up into the Faddeev equation for a T operator given by

$$T = tP + tPG_0T. \tag{4}$$

The transition operator U_0 for the breakup process is then

$$U_0 = (1+P)T. \tag{5}$$

Equation (4) is solved numerically for any given NN force which determines the two-nucleon off-shell t matrix, t. G_0 is the $3N$ free propagator and the identity of the nucleons (working in isospin formalism) is accounted for by the permutation operator P whose two parts, a cyclic and an anticyclic permutation, are responsible for the respective exchanges of the nucleons.

The matrix elements of U_0 between the incoming state $|\phi\rangle$, which is composed of the deuteron wave function φ_d and the momentum eigenstate of the free nucleon-deuteron motion $|\vec{q}_0\rangle$, and the final state, determine the breakup cross section. Kinematically-complete breakup configurations are fixed by the standard Jacobi momenta $\vec{p}$ and $\vec{q}$. In order to evaluate the energy spectrum of the outgoing neutron, a proper integration over all kinematically-complete configurations contributing to a given energy must be carried through [21]. For details of the theoretical formalism and the numerical performance we refer to Refs. [5,22,23].

The calculations presented here use the Bonn B NN potential [17]. All partial wave components of the force were kept up to a total two-nucleon angular momentum $j_{\max}=3$. The results are compared to the data in Fig. 3. It is seen that both the FSI peak at forward angles and the QFS peak at larger angles show up, and give a good account of the experimental energy and angle dependence without the ambiguities inherent in the separate IA-FSI and QFS estimates of Sec. IV that have long been necessary to describe breakup at these energies; however, this is not surprising because the Faddeev theory is an exact treatment and should therefore account for all aspects of processes induced by the nucleon-deuteron interaction.

In spite of the success of our Faddeev calculations in describing both the FSI and QFS peaks, it is clearly seen in Fig. 3 that the FSI peak is not described very well. The calculations predict a peak which is too narrow and too strong. We ascribe this discrepancy to the fact that our three-body calculations do not include the Coulomb force acting between the two protons. Exact inclusion of the long range Coulomb force together with realistic NN interactions is a notorious problem for present day $3N$ calculations above the deuteron breakup threshold. Only recently has a first attempt been made [24] which, however, still uses only a rank one separable Yamaguchi force. One has to expect that especially in

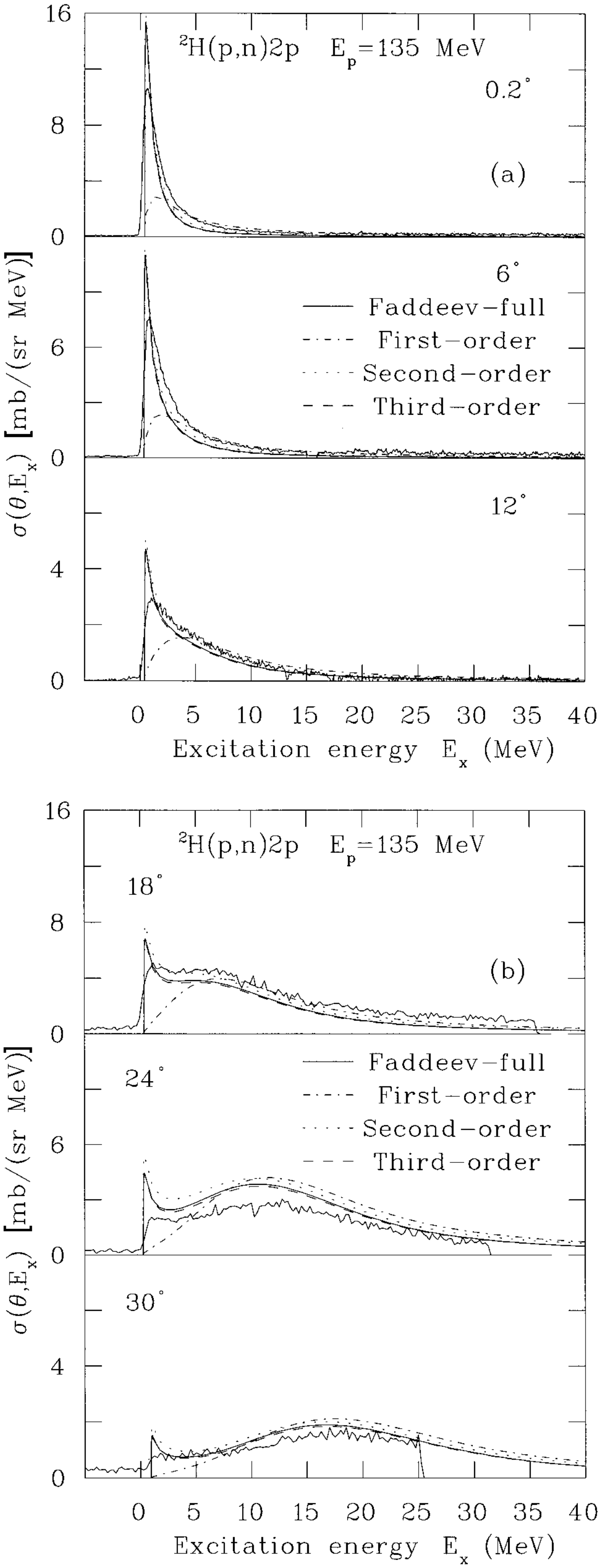

FIG. 3. Comparison of three-body Faddeev calculations for the ^{2}H(p,n) reaction (solid line) with the experimental excitation-energy spectra at (a) 0.2°, 6°, and 12°, and (b) 18°, 24°, and 30°. The importance of the rescattering terms of various orders in t are also shown: first order in t (dashed-dotted), up to second order in t (dotted), and up to third order in t (dashed).

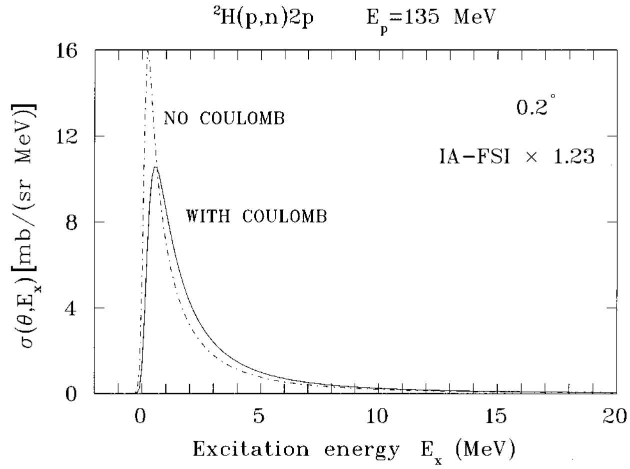

FIG. 4. Comparison of FSI impulse-approximation calculations with and without Coulomb interaction in the final-state wave function at 0.2°.

the region of the final-state interaction peak at the low energy part of the neutron spectrum where two protons leave the interaction region with approximately equal momenta, the Coulomb force is important. This has been confirmed by turning the Coulomb interaction on and off in the FSI-IA calculations of Sec. IV. We show these calculations, compared with the 0.2° spectrum, in Fig. 4. The effect of the Coulomb interaction is a destructive interference which broadens the final-state interaction peak in just the right way so as to reproduce the experimental FSI spectrum well.

Assuming that Coulomb effects are confined to the FSI region, the Faddeev calculations can be said to describe the complete experimental spectrum fairly well. In the quasifree region of the spectra, one sees that the Faddeev calculations somewhat underestimate the cross section at forward angles and somewhat overestimate the cross section at wider angles. This difference is most pronounced in the 24° spectrum. This difficulty may be due in part to not taking into account relativistic effects, which at this energy may be non-negligible.

We would like to add remarks here on the importance of rescattering terms beyond the first-order term in the two-nucleon t matrix. It might be expected that rescattering affects the different portions of the neutron energy spectrum differently.

Iterating Eq. (4) one obtains the multiple scattering series

$$T = tP + tPG_0tP + tPG_0tPG_0tP + \cdots \tag{6}$$

with terms of different order in the t matrix, whose magnitudes depend on the incoming energy and on the particular kinematically-complete configuration of the three outgoing nucleons under study. The QFS-IA calculation of Sec. IV is produced if only the first term, $T \approx tP$, is retained to construct the breakup transition operator U_0. Then the breakup amplitude is

$$\begin{aligned}\langle \phi_0 | (1+P)T | \phi \rangle &\approx \langle \phi_0 | (1+P)tP | \phi \rangle \\ &= \langle \phi_0 | t_1 | \phi \rangle_2 + \langle \phi_0 | t_1 | \phi \rangle_3 + \langle \phi_0 | t_2 | \phi \rangle_3 \\ &\quad + \langle \phi_0 | t_2 | \phi \rangle_1 + \langle \phi_0 | t_3 | \phi \rangle_1 + \langle \phi_0 | t_3 | \phi \rangle_2 .\end{aligned} \tag{7}$$

The indices at the ket vectors denote the singled-out nucleon which carries the relative momentum $\vec{q}_0$ in the incoming channel state $|\phi\rangle = |\varphi_d\rangle|\vec{q}_0\rangle$. Because of the antisymmetry of $|\varphi_d\rangle$, this can be written more compactly as

$$\langle\phi_0|(1+P)tP|\phi\rangle = \langle\phi_0|(1-P_{23})t_1|\phi\rangle_2 + \langle\phi_0|(1-P_{13})t_2|\phi\rangle_3 + \langle\phi_0|(1-P_{12})t_3|\phi\rangle_1 . \tag{8}$$

It is also a fairly easy exercise to evaluate this further with the result

$$\begin{aligned}\langle\phi_0|(1+P)tP|\phi\rangle = &\sum_{m_3'\nu_3'} {}_a\left\langle \vec{p}m_2m_3\nu_2\nu_3\left|t\left(E-\frac{3}{4m}\vec{q}^{\,2}\right)\right|\vec{q}_0+\frac{1}{2}\vec{q}m_Nm_3'\nu_N\nu_3'\right\rangle\left\langle -\frac{1}{2}\vec{q}_0-\vec{q}m_3'm_1\nu_3'\nu_1\middle|\varphi_d\right\rangle \\ &+\sum_{m_1'\nu_1'} {}_a\left\langle -\frac{1}{2}\vec{p}-\frac{3}{4}\vec{q}m_1m_3\nu_1\nu_3\left|t\left[E-\frac{3}{4m}\left(\vec{p}-\frac{1}{2}\vec{q}\right)^2\right]\right|\frac{1}{2}\vec{p}+\vec{q}_0-\frac{1}{4}\vec{q}m_1'm_N\nu_1'\nu_N\right\rangle \\ &\times\left\langle -\vec{p}+\frac{1}{2}\vec{q}-\frac{1}{2}\vec{q}_0m_1'm_2\nu_1'\nu_2\middle|\varphi_d\right\rangle + \sum_{m_2'\nu_2'} {}_a\left\langle -\frac{1}{2}\vec{p}+\frac{3}{4}\vec{q}m_1m_2\nu_1\nu_2\left|t\left[E-\frac{3}{4m}\left(\vec{p}+\frac{1}{2}\vec{q}\right)^2\right]\right.\right. \\ &\times\left.\left| -\frac{1}{2}\vec{p}+\vec{q}_0-\frac{1}{4}\vec{q}m_Nm_2'\nu_N\nu_2'\right\rangle\left\langle \vec{p}+\frac{1}{2}\vec{q}-\frac{1}{2}\vec{q}_0m_2'm_3\nu_2'\nu_3\middle|\varphi_d\right\rangle,\end{aligned} \tag{9}$$

where $|\vec{p}m_2m_3\nu_2\nu_3\rangle_a \equiv (1-P_{23})|\vec{p}m_2m_3\nu_2\nu_3\rangle$ is a properly antisymmetrized state with P_{23} the corresponding exchange operator. The c.m. energy of the $3N$ system E is related to the initial nucleon-deuteron relative momentum $\vec{q}_0$ in the channel $|\phi\rangle$ and shows up again in the two kinetic energies of relative motion

$$E = \frac{3}{4m}\vec{q}_0^{\,2} + \epsilon_d = \frac{1}{m}\vec{p}^{\,2} + \frac{3}{4m}\vec{q}^{\,2}, \tag{10}$$

where ϵ_d is the binding energy of the deuteron.

Under the FSI condition, $\vec{k}_2^{\rm lab} = \vec{k}_3^{\rm lab}$, one has

$$\vec{p} = 0,$$

$$\vec{q} = \frac{2}{3}(\vec{k}_1^{\rm lab} - \vec{k}_2^{\rm lab}),$$

$$\vec{q}_0 = \frac{2}{3}(\vec{k}_1^{\rm lab} + 2\vec{k}_2^{\rm lab}). \tag{11}$$

Then the energy arguments of the t matrices appearing in Eq. (9) are exactly equal to zero for the first, and $(1/4m)\vec{k}_{\rm lab}^2 + \frac{3}{4}\epsilon_d$ for the second and third terms, respectively, where $\vec{k}_{\rm lab}$ is the laboratory momentum of the incoming nucleon. The arguments of the corresponding deuteron states appearing in Eq. (9) are $-\vec{k}_1^{\rm lab}$ for the first and $-\vec{k}_2^{\rm lab}$ for the second and third terms, respectively. Thus only in the first term is the two-nucleon t matrix close to the $^1S_0$ virtual pole and favors a FSI peak in the outgoing neutron spectrum; however, at our high incoming energy the contribution of this term is drastically reduced by the fact that a large argument occurs in the corresponding deuteron wave function. Therefore this first order term in t contributes to high outgoing neutron energy only via a nucleon exchange process and will create no strong final state interaction peak. In order to create a strong FSI, at least the second order term in t is required. This is also in agreement with the considerations of Sec. IV, where in Eqs. (1) and (2) the np cross section and the two-nucleon scattering state for the two final protons occur. This is based on a second order process in t. Now for quasifree scattering conditions, for instance $\vec{k}_1^{\rm lab} = 0$, one has $\vec{q} = -\frac{1}{2}\vec{q}_0$, which puts the argument of the deuteron state in the first term to zero. At the same time the two-nucleon t matrix is close to being on shell (up to ϵ_d corrections). The other two terms are suppressed. This leads to the QFS bump, as has been known for a long time.

We display in Fig. 3 the breakup cross section based on the breakup amplitude U_0 evaluated to various orders in t. It is seen clearly that at our energy only after inclusion of second order rescatterings does the FSI peak appear in the outgoing neutron spectrum. It is necessary to add then the third order rescatterings in order to reproduce the FSI peak of the full solution. At higher excitation energies rescatterings are also important, even in the bump region because in this kinematically-incomplete spectrum a lot of different breakup configurations contribute at a specific neutron energy.

VI. CONCLUSIONS

We measured cross section excitation-energy spectra for the ^{2}H$(p,n)2p$ reaction at 135 MeV in 6° steps from 0° to 30° (laboratory). The energy resolution was 260 keV. These measurements have better resolution by more than a factor of 2 and extend to wider angles than previous experiments performed to study this reaction above 100 MeV. The spectra are dominated by the $^1S_0$ final-state interaction (FSI) peak observed at low excitation energy in the residual $2p$ system at forward angles. The broad quasifree scattering (QFS) peak is clearly seen moving to higher excitation energy with increasing angle.

The experimental spectra are compared with impulse-approximation (IA) and rigorous three-body Faddeev calculations. Separate FSI-IA and QFS-IA calculations were performed which describe the FSI peak and the QFS peak, respectively, both with normalization factors near unity; however, the separate estimates for the almost distinct mechanisms, that have long been necessary for breakup at these higher energies, limits the quantitative understanding of the reaction. Three-body Faddeev calculations yield both features simultaneously and remove this limitation as well as provide a good description of the data. These calculations do not include the Coulomb force between the two final state interacting protons and thus do not describe the shape of the FSI peak as well as the FSI-IA calculations, performed with the pp Coulomb force included. Although it is not now possible to include exactly the Coulomb force into three-body calculations above the deuteron breakup threshold, we see by turning the Coulomb off and on in the FSI-IA calculations that this is likely to account for the discrepancy observed at forward angles in the three-body calculations. The Faddeev calculations also somewhat overestimate the data in the QFS region at wider angles. This discrepancy is not understood but may be due in part to the neglect of relativisitic effects in the calculations.

Future experiments are planned to measure a complete set of spin observables for this reaction. They may be sensitive to three-body force effects and to the D-state contribution in the deuteron wave function and thus will provide additional tests of $3N$ continuum Faddeev calculations at high energies.

ACKNOWLEDGEMENTS

We would like to thank the staff of the Indiana University Cyclotron Facility for their help in mounting and running this experiment. This work was supported in part by the National Science Foundation and by the Polish-American Maria-Skłodowska-Curie II FUND under Grant No. MEN/NSF-94-161. The numerical calculations have been performed on the Cray Y-MP of the Höchstleistungsrechenzentrum in Jülich, Germany.

[1] A. Langsford, P.H. Bowen, G.C. Cox, P.E. Dolly, R.A.J. Riddle, and M.J.M Saltmarsh, Nucl. Phys. **A99**, 246 (1967).
[2] A.S. Clough, C.J. Batty, B.E. Bonner, C. Tashalar, and L.E. Williams, Nucl. Phys. **A121**, 689 (1968).
[3] H. Sakai, T.A. Carey, J.B. McClelland, T.N. Tadduecci, R.C. Byrd, C.D. Goodman, D. Krofcheck, L.J. Rybarcyk, E. Sugarbaker, A.J. Wagner, and J. Rapaport, Phys. Rev. C **35**, 344 (1987).
[4] D.J. Mercer, T.N. Taddeucci, L.J. Rybarcyk, X.Y. Chen, D.L. Prout, R.C. Byrd, J.B. McClelland, W.C. Sailor, S. DeLucia, B. Luther, D.G. Marchlenski, E. Sugarbaker, I. Gulmez, Jr., C.D. Goodman, and J. Rappaport, Phys. Rev. Lett. **71**, 684 (1993).
[5] H. Witala, Th. Cornelius, and W. Glöckle, Few-Body Syst. **3**, 123 (1988).
[6] H. Witala, W. Glöckle, and Th. Cornelius, Few-Body Syst. **6**, 79 (1989).
[7] W. Glöckle, H. Witała, H. Kamada, D. Hüber, and J. Golak, in *Few Body Problems in Physics*, Williamsburg, 1994, edited by F. Gross, AIP Conf. Proc. No. 334 (AIP Press, New York, 1995), p. 45.
[8] B.D. Anderson, T. Chrittrakarn, A.R. Baldwin, C. Lebo, R. Madey, P.C. Tandy, J.W. Watson, B.A. Brown, and C.C. Foster, Phys. Rev. C **31**,1161 (1985).
[9] B.D. Anderson, N. Tamimi, A.R. Baldwin, M. Elaasar, R. Madey, D.M. Manley, M. Mostajabodda'vati, J.W. Watson, W.M. Zhang, and C.C. Foster, Phys. Rev. C **43**, 50 (1991).
[10] A.R. Baldwin and R. Madey, Nucl. Instrum. Methods **171**, 149 (1980).
[11] R. Madey *et al.*, Nucl. Instrum. Methods **214**, 401 (1983).
[12] R. Cecil, B.D. Anderson, and R. Madey, Nucl. Instrum. Methods **161**, 439 (1979).
[13] J.W. Watson, B.D. Anderson, A.R. Baldwin, C. Lebo, B. Flanders, W. Pairsuwan, R. Madey, and C.C. Foster, Nucl. Instrum. Methods **215**, 413 (1983).
[14] J. D'Auria, M. Dombsky, L. Moritz, T. Ruth, G. Sheffer, T.E. Ward, C.C. Foster, J.W. Watson, B.D. Anderson, and J. Rapaport, Phys. Rev. C **30**, 1999 (1984).
[15] R.J.N. Phillips, Nucl. Phys. **53**, 650 (1964).
[16] R.A. Arndt, computer code SAID (unpublished).
[17] R. Machleidt, K. Holinde, and Ch. Elster, Phys. Rep. **149**, 1 (1987); R. Machleidt, Adv. Nucl. Phys. **19**, 189 (1989).
[18] B.D. Anderson, A.R. Baldwin, A.M. Kalenda, R. Madey, J.W. Watson, C.C. Chang, H.D. Holmgren, R.W. Koontz, and J.R. Wu, Phys. Rev. Lett. **46**, 226 (1981).
[19] J.R. Wu, Phys. Lett. **91B**, 169 (1980).
[20] N.S. Chant (private communication).
[21] J. Balewski, K. Bodek, L. Jarczyk, B. Kamys, St. Kistryn, A. Strzałkowski, W. Hajdas, R. Müller, B. Dechant, J. Krug, W. Lübcke, H. Rühl, G. Spangardt, M. Steinke, M. Stephan, D. Kamke, R. Henneck, H. Witała, W. Glöckle, and J. Golak, Nucl. Phys. **A581**, 131 (1995).
[22] W. Glöckle, *The Quantum-Mechanical Few-Body Problem* (Springer-Verlag, Berlin-Heidelberg 1983).
[23] W. Glöckle, in *Models and Methods in Few-Body Physics*, edited by L. S. Ferreira, A. C. Fonseca, and L. Streit, Lecture Notes in Physics Vol. 273 (Springer-Verlag, Berlin, 1987), p. 3.
[24] E.O. Alt and M. Rauch, Few-Body Syst. Suppl. 7, 160 (1994).